Polarization-Dependent Confinement Losses in Actual Holey Fibers

Masanori Koshiba, *Fellow, IEEE,* and Kunimasa Saitoh, *Member, IEEE*

***Abstract*—Through the real-model simulations, the polarization-dependent confinement losses in actual holey fibers are, for the first time, numerically demonstrated. Furthermore, it is confirmed that the interstitial holes caused by the packing of the capillaries play a role to significantly reduce the confinement losses.**

***Index Terms*—Confinement loss, holey fiber (HF), photonic crystal fiber.**

I. Introduction

PHOTONIC CRYSTAL fibers [1], also called holey fibers (HFs) [2], consisting of a central defect region surrounded by air holes running parallel to the fiber length have been one of the most interesting development in recent fiber optics. By varying the size of the holes and their number and position, the dispersive and modal properties could be easily controlled. HFs are usually made from pure silica, and so the guided modes are inherently leaky because the core index is the same as the index of the outer cladding region without air holes.

Recently, the multipole method (MM) has been effectively applied to investigating the confinement losses in HFs [3], [4]. Although the MM can describe leaky nature of HFs with finite number of air holes and can give accurate results for both the real and the imaginary parts of the propagation constants, it is difficult to deal with noncircular air holes which appear frequently in actual fiber structures [4], [5]. In the MM, therefore, all the air holes are replaced by the circular ones and some of the interstitial holes and outer holes are usually neglected [4]. More recently, a full-vector finite element method (FEM) using perfectly matched layers (PMLs) as absorbing boundary conditions has also been introduced to predict the confinement losses in HFs [6]. In [6], however, only the canonical structures, HFs with six-fold rotational symmetry, are treated.

In this letter, the finite element simulations are performed for HFs and the polarization-dependent confinement losses in actual fiber structures are, for the first time, numerically demonstrated. In addition, it is confirmed that interstitial holes caused by the packing of the capillaries play a role to significantly reduce the confinement losses.

II. Confinement Losses

First, to check the accuracy of the full-vector FEM, Fig. 1(a) and (b) shows, respectively, the confinement losses in HFs with two and three rings of arrays of air holes as a function of hole pitch Λ, where d is the hole diameter and the operating wavelength is assumed to be 1.55 μm. Our results agree well with those of the full-vector MM [4], showing the reliability of the full-vector FEM with PMLs.

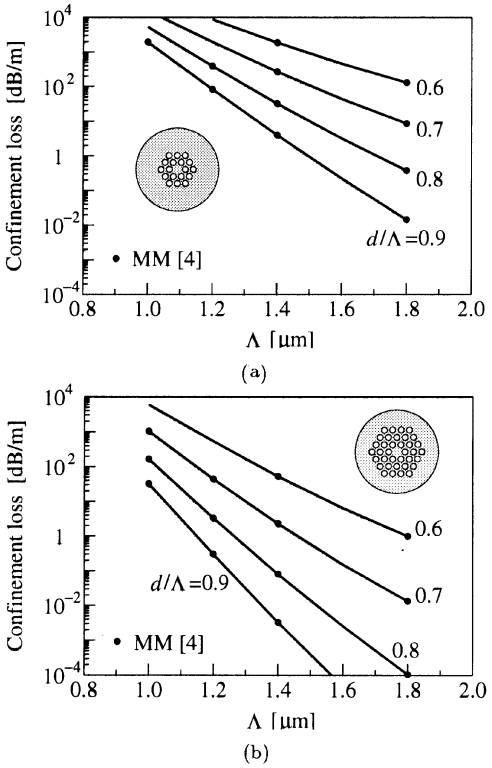

Fig. 1. Confinement losses in HFs with (a) two and (b) three rings of arrays of air holes.

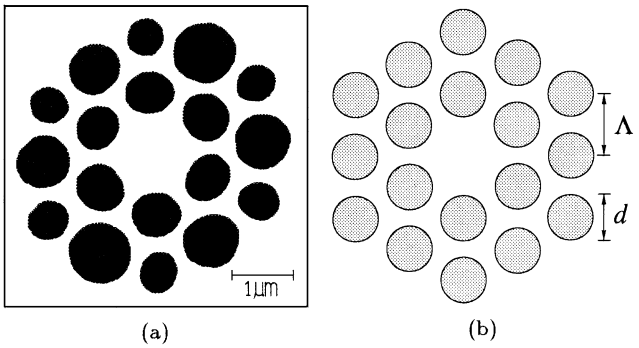

Fig. 2. (a) Real and (b) idealized models for HFs with two rings of arrays of air holes.

Next, we consider an actual HF with two rings of arrays of air holes as shown in Fig. 2(a) [5]. Fig. 2(b) shows the corresponding idealized structure with six-fold rotational symmetry,

Manuscript received October 1, 2002; revised January 3, 2003.

The authors are with the Division of Electronics and Information Engineering, Graduate School of Engineering, Hokkaido University, Sapporo 060-8628, Japan.

Digital Object Identifier 10.1109/LPT.2003.809923

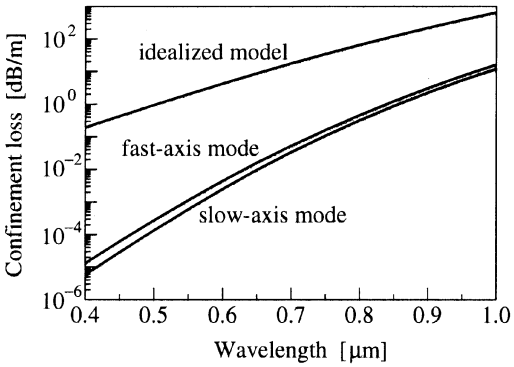

Fig. 3. Confinement losses in HFs with two rings of arrays of air holes.

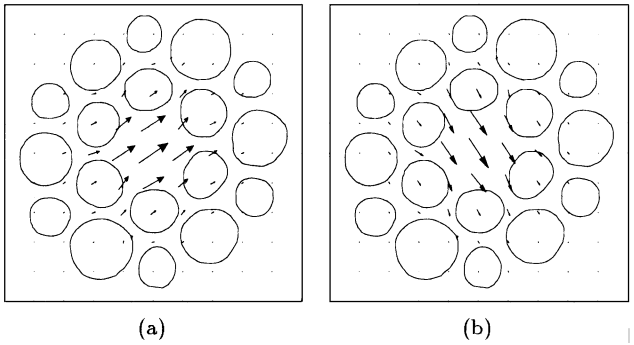

Fig. 4. Transverse electric-field vector distributions of (a) slow-axis and (b) fast-axis modes in a real HF shown in Fig. 2(a).

where the hole pitch $\Lambda = 1.0$ μm and the hole diameter $d = 0.62$ μm suggested in [5]. The background refractive index is assumed to be 1.45.

Fig. 3 shows the confinement losses of the two linearly polarized fundamental modes called slow-axis and fast-axis modes as a function of wavelength. The real part of effective index of the slow-axis mode is slightly larger than that of the fast-axis mode. The transverse electric-field vector distributions of the slow-axis and fast-axis modes at the wavelength of 1.0 μm are, respectively, shown in Fig. 4(a) and (b). In Fig. 3, the results for the corresponding idealized structure [5] are also plotted. In the idealized structure, the two fundamental modes are degenerate [7], [8], and so the confinement losses are independent of the polarization states. In the actual fiber structure, on the other hand, it is confirmed that the confinement losses depend on the polarization state and that the losses of the fast-axis mode are slightly larger than those of the slow-axis mode. As described above, the real part of effective index of the fast-axis mode is smaller than that of the slow-axis mode and, therefore, the former field is less confined within the core region compared with the latter one. The losses of the real model are quite smaller than those of the idealized model. In the actual fiber structure [5], there are some relatively large air holes with diameter of 1 μm or so [see Fig. 2(a)], and, therefore, the refractive-index difference between the core and the air-holes cladding regions becomes larger, resulting in the confinement-loss reduction in the real model.

Last, we consider another actual HF with interstitial holes as shown in Fig. 5(a) [4]. Fig. 5(b) shows a simplified model according to [4], where some of the interstitial and outer holes are removed from the original structure in Fig. 5(a). In [4], in order to apply the MM, the circular holes arrangement in Fig. 5(c) has been chosen to provide the best match to the real HF structure in Fig. 5(a).

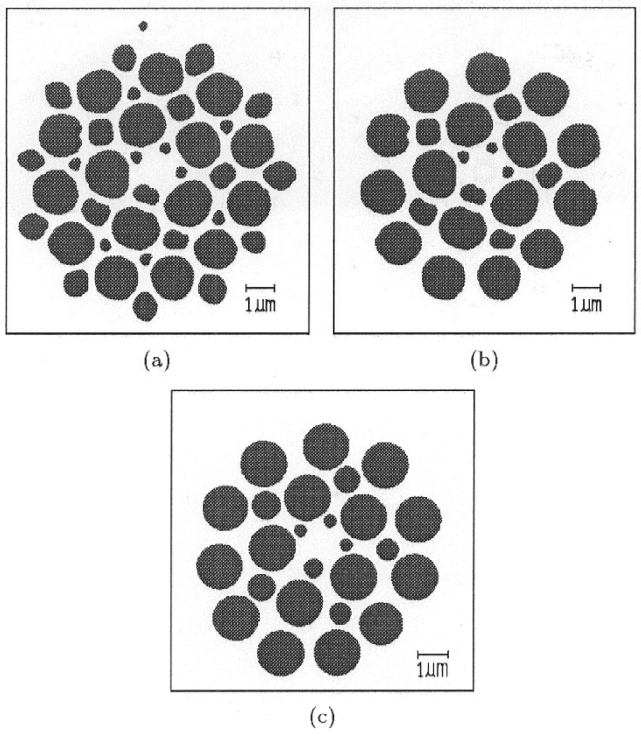

Fig. 5. (a) Original, (b) simplified, and (c) circular models for HFs with interstitial holes.

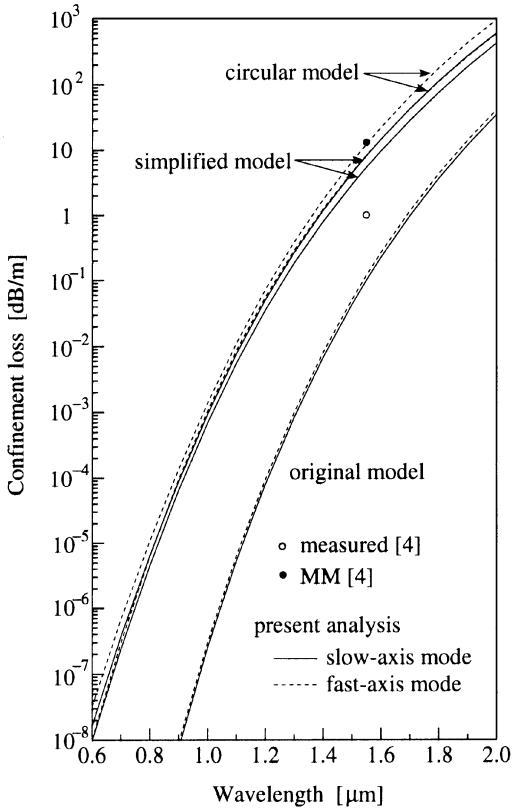

Fig. 6. Confinement losses in HFs with interstitial holes.

Fig. 6 shows the confinement losses of the slow-axis and fast-axis modes as a function of wavelength. The transverse

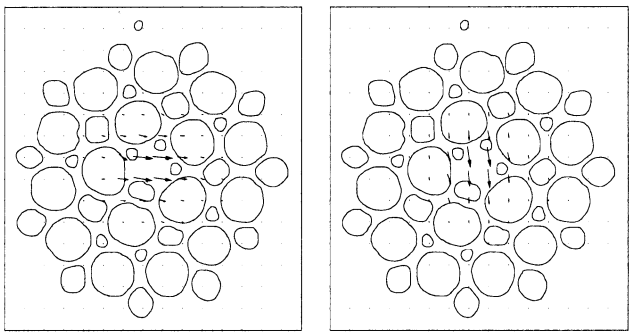

Fig. 7. Transverse electric-field vector distributions of (a) slow-axis and (b) fast-axis modes in a real HF shown in Fig. 5(a).

electric-field vector distributions of the slow-axis and fast-axis modes at the wavelength of 1.55 μm are, respectively, shown in Fig. 7(a) and (b). The difference in the confinement losses between these two fundamental modes is very small for the original structure in Fig. 5(a). Removing some interstitial holes as in Fig. 5(b), the confinement losses increase rapidly, especially in short-wavelength region. At the wavelength of 1 μm, for example, the confinement loss is less than 10^{-6} dB/m $=$ 0.001 dB/km for the original structure in Fig. 5(a), while that is about 1 dB/km for the simplified structure in Fig. 5(b). We can say that the interstitial holes play an important role to significantly reduce the confinement losses. It seems that the interstitial holes have the effects of increasing the number of air-holes rings and/or the refractive-index difference between the core and the air-holes cladding regions. The results obtained for the further simplified circular model in Fig. 5(c) are almost the same as those for the previous structure with noncircular air holes in Fig. 5(b), showing the validity of replacing noncircular air holes by the corresponding circular ones.

Table I shows the confinement losses at the wavelength of 1.55 μm. We can see again that the confinement losses are reduced with increasing number of interstitial air holes. The calculated confinement losses for the original structure in Fig. 5(a) are considerably small, compared with the measured value of 1 dB/m [4]. This seems to be due to the fact that in our calculation, the other loss mechanisms such as material loss and/or waveguide imperfection loss, are not included. For the circular model in Fig. 5(c), the results of FEM agree approximately with those of MM [4].

TABLE I
CONFINEMENT LOSSES AT WAVELENGTH OF 1.55 μm

method	structure	slow-axis	fast-axis
FEM	Fig. 5 (a)	0.099 dB/m	0.118 dB/m
	Fig. 5 (b)	5.36 dB/m	8.23 dB/m
	Fig. 5 (c)	8.11 dB/m	12.2 dB/m
MM [4]	Fig. 5 (c)	13 dB/m	
measured [4]	Fig. 5 (a)	$\sim$ 1 dB/m	

III. CONCLUSION

Through the real-model simulations, polarization-dependent confinement losses in actual HFs have been numerically demonstrated. Also, it was confirmed that the interstitial holes play a role to significantly reduce the confinement losses.

REFERENCES

[1] J. C. Knight, T. A. Birks, P. St. J. Russell, and D. M. Atkin, "All-silica single-mode optical fiber with photonic crystal cladding," *Opt. Lett.*, vol. 21, pp. 1547–1549, Oct. 1996.
[2] P. J. Bennett, T. M. Monro, and D. J. Richardson, "Toward practical holey fiber technology: Fabrication, splicing, modeling, and characterization," *Opt. Lett.*, vol. 24, pp. 1203–1205, Sept. 1999.
[3] T. P. White, R. C. McPhedran, C. M. de Sterks, L. C. Botten, and M. J. Steel, "Confinement losses in microstructured optical fibers," *Opt. Lett.*, vol. 26, pp. 1660–1662, Nov. 2001.
[4] V. Finazzi, T. M. Monro, and D. J. Richardson, "Confinement loss in highly nonlinear holey optical fibers," in *Proc. Opt. Fiber Commun. Conf.*, Anaheim, CA, 2002, Paper ThS4.
[5] J. C. Knight, J. Arriaga, T. A. Birks, A. Ortigosa-Blanch, W. J. Wadsworth, and P. St. J. Russell, "Anomalous dispersion in photonic crystal fiber," *IEEE Photon. Technol. Lett.*, vol. 12, pp. 807–809, July 2000.
[6] K. Saitoh and M. Koshiba, "Full-vectorial imaginary-distance beam propagation method based on finite element scheme: Application to photonic crystal fibers," *IEEE J. Quantum Electron.*, vol. 38, pp. 927–933, July 2002.
[7] M. J. Steel, T. P. White, C. Martijn de Sterke, R. C. McPhedran, and L. C. Botten, "Symmetry and degeneracy in microstructured optical fibers," *Opt. Lett.*, vol. 26, pp. 488–490, Apr. 2001.
[8] M. Koshiba and K. Saitoh, "Numerical verification of degeneracy in hexagonal photonic crystal fibers," *IEEE Photon. Technol. Lett.*, vol. 13, pp. 1313–1315, Dec. 2001.